

# Vibrational Energy Relaxation of “Tailored” Hemes in Myoglobin Following Ligand Photolysis Supports Energy Funneling Mechanism of Heme “Cooling”

Lintao Bu and John E. Straub\*

Department of Chemistry, Boston University, Boston, Massachusetts 02215

Received: March 4, 2003; In Final Form: July 7, 2003

In a previous molecular dynamics simulation study, the kinetic energy relaxation of photolyzed heme in solvated carbonmonoxymyoglobin was found to be a single exponential decay process with the relaxation time constant 5.9 ps [Sagnella, D. E.; Straub, J. E. *J. Phys. Chem. B* **2001**, *105*, 7057]. The strong electrostatic interaction of the isopropionate side chains and the solvating water molecules was shown to be the single most important “doorway” for dissipation of excess kinetic energy in the heme. In this work, the results of a molecular dynamics simulation study of heme “cooling” in two modified myoglobins, in which (1) the two isopropionate side chains in the heme are replaced by hydrogen or (2) the proximal histidine is replaced by glycine, His93Gly, are presented. For each “tailored” protein, the relaxation of the heme’s excess kinetic energy is found to be a single exponential decay process. For the His93Gly mutant protein, the relaxation time is found to be 5.9 ps, in agreement with the relaxation time in native wild-type myoglobin. For myoglobin with the modified heme lacking isopropionate side chains, the relaxation time was found to be 8.8 ps—a decrease by 50% compared to that for native myoglobin. These results lend strong support to the proposal that the predominant channel for fast kinetic energy relaxation of the heme in native myoglobin is directed energy “funneling” through the heme side chains to the surrounding solvent.

## 1. Background

Following ligand binding or dissociation, heme proteins undergo vibrational energy relaxation (VER). Understanding the time scales and mechanisms of vibrational energy transfer is an essential component of a complete understanding of the ultrafast conformational changes and the reorganization of protein structures that follow fundamental events such as binding or release of substrate molecules, or electron transfer.<sup>1–7</sup>

Much experimental and theoretical work has been done to investigate the rate of vibrational energy relaxation for small diatomic ligands,<sup>8–14</sup> particularly CO in the heme protein myoglobin.<sup>15–17</sup> In myoglobin, ligand dissociation can occur when the ligand–heme complex absorbs a visible or UV photon, which can cause vibrational excitation of the ligand, heme, and surrounding residues<sup>18,19</sup> and a global conformational transformation of the protein. The detailed analysis of vibrational energy relaxation of heme proteins can provide important information about the cooperative nature of protein dynamics.<sup>8</sup>

Computer simulation of vibrational energy relaxation in heme proteins began with the pioneering work of Hochstrasser and co-workers.<sup>20</sup> By adding 54 or 81 kcal/mol of kinetic energy to the heme, they simulated the process of absorption of a 530 or 353 nm photon. They found the heme “cooling” in the heme proteins myoglobin and cytochrome *c* to be a biphasic process with roughly 50% energy loss occurring in 1–4 ps in a “fast” process attributed to relaxation by “collective modes”<sup>21</sup> and the remainder in 20–40 ps by a “slow” process attributed to heat diffusion in the protein. Their simulation work was done in vacuo; they argued that the solvent may increase the relaxation rate. In myoglobin, much of the heme is buried in a hydrophobic pocket within the protein matrix, but the heme has significant contacts with the solvent. The two isopropionate side chains of the heme are highly solvated and extend away from the protein.

Hochstrasser first suggested the possibility that the vibrational energy could be transferred directly from the heme to the solvent through the two heme isopropionate side chains.<sup>20,21</sup>

Time-resolved Raman studies by Martin and co-workers<sup>22</sup> found that the heme’s excess energy, following excitation by a 500 nm pulse, is transferred to protein modes in approximately 5 ps. In a related study of deoxyhemoglobin, Lingle and co-workers found the heme’s excess vibrational energy to dissipate within 15 ps.<sup>23</sup> From a Raman scattering study on a variety of metalloproteins, Li, Sage, and Champion derived a time constant for heme cooling of 4 ps.<sup>24</sup> Lim, Jackson, and Anfinrud reported a single-exponential time constant of  $6.2 \pm 0.5$  ps for cooling of the electronically relaxed heme.<sup>35</sup> Kitagawa and co-workers monitored the time dependence of the relaxation of an excited in-plane vibrational mode of the heme in myoglobin using resonance Raman spectroscopy, concluding that the decay was biphasic with time constants of  $3.0 \pm 1.0$  ps (for 93% of the relaxation) and  $25.0 \pm 14.0$  ps.<sup>10</sup> The results of each of those studies is consistent with a view of a significant component of the heme vibrational relaxation occurring on a time scale of 3–5 ps.

Subsequently, Sagnella and Straub<sup>25,26</sup> studied the heme “cooling” in solvated myoglobin using molecular dynamics simulation. To simulate the photolysis process, approximately 88 kcal/mol of excess of kinetic energy, equivalent to two 650 nm photons, was deposited in the heme. They found evidence for energy transfer from the heme to the surrounding protein and solvent proceeding through three channels: “through projectile” involving ligand collisions with the heme pocket residues, “through bond” involving covalent bond between heme and proximal histidine, and “through space” involving non-bonded collision channels. Most significantly, they found strong evidence for the mechanism of “highly directly energy funneling” suggested by Hochstrasser and co-workers.<sup>21</sup> Sagnella and

Straub identified the dominant channel for vibrational energy relaxation of the heme to be one involving two steps: (1) the excess kinetic energy is redistributed through a rapid intraheme vibrational relaxation process and (2) the excess kinetic energy is transferred to the surrounding solvent directly through the two isopropionate side chains. The simulation results indicate that the heme’s kinetic energy relaxed according to a single-exponential process with a time constant of roughly 5.9 ps. That theoretical result agrees with the experimental result of Lim, Jackson, and Anfinrud, who observed heme “cooling” in myoglobin to be a single-exponential process with a time constant of  $6.2 \pm 0.5$  ps.<sup>12</sup>

In this paper, we present our computational study of the heme relaxation process in two tailored myoglobins—the His93Gly mutant with native heme *b* and wild-type myoglobin in which the two isopropionate side chains in the heme are each replaced by hydrogen atoms. If the energy transfer channel through the two isopropionate side chains is the dominant channel for heme “cooling” as has been proposed, one expects to see a significant variation in the relaxation rate for heme “cooling” in a heme without its acidic side chains. However, little change in the relaxation rate is expected for the His93Gly mutant with native heme *b*—its acidic side chains are intact. Our simulation results provide direct support for this view and a detailed picture of the pathways for energy flow from excited hemes in myoglobin.

## 2. Computational Model and Methods

**2.1. Molecular Dynamics.** The computational protocol follows closely that developed by Sagnella and Straub.<sup>26</sup> The sperm whale myoglobin molecule and solvent water were introduced into a  $56.70 \times 56.70 \times 37.712$  Å<sup>3</sup> box and simulated using the CHARMM program.<sup>27</sup> The initial configuration of the system, including protein, heme, and solvent, was equilibrated at room temperature as part of a previous study.<sup>26</sup> The all-hydrogen parameter set (version 27) of the CHARMM<sup>28</sup> force field was used.

In His93Gly mutant myoglobin, the His93 was replaced by Gly93, with the resulting heme being five-coordinate in the A-state. One molecular dynamics trajectory was run for 30 ps at constant energy until the new equilibrium state for the His93Gly mutant myoglobin was reached. Subsequently, one molecular dynamics trajectory was run for 50 ps at constant energy and volume. During equilibration, the velocities were randomly resampled according to the Maxwell distribution to maintain a constant temperature. The molecular dynamics employed the Verlet algorithm, which is time reversible and symplectic.<sup>29–31</sup> The nonbonded Lennard-Jones and electrostatic potential energy was truncated using a group based switching function extending from 9.5 to 11.5 Å. Snapshot configurations were saved every 5 ps. For each of the 10 configurations obtained in this way, 30 ps trajectories were run for both the equilibrium initial states and nonequilibrium excited states. The initial configuration for each excited state was identical to the corresponding nonexcited state at the moment of excitation with the exception of the velocities of the 73 heme atoms.

In myoglobin with the modified heme, the heme’s two isopropionate side chains were amputated and replaced by hydrogen atoms. Figure 1a shows the structure of the heme for native myoglobin, and Figure 1b shows the structure of the modified heme used in this study. One molecular dynamics trajectory was run for 20 ps at constant energy until the new equilibrium state for this modified myoglobin was reached. The following molecular dynamics simulation protocol is that used in the simulations of the His93Gly mutant protein.

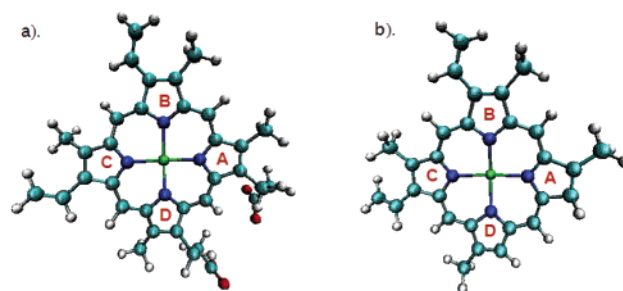


**Figure 1.** (a) Structure of heme for wild-type/His93Gly mutant myoglobin, in which the positions of two isopropionate side chains can be seen. (b) Structure of heme for the modified myoglobin, in which the two isopropionate side chains are amputated and replaced by two hydrogen atoms (green, Fe; blue, N; red, O; cyan, C; white, H).

**2.2. Preparation of the Excited State.** To simulate the absorption of a photon, approximately 88 kcal/mol of excess kinetic energy, equivalent to two 650 nm photons, was deposited in the heme. The excess kinetic energy was distributed uniformly among the heme atoms. With the excess kinetic energy equipartitioned to the vibrational modes of the heme, the “temperature” of the heme would increase by 400 K for the His93Gly mutant and 500 K for the modified heme mutant.

In the photolyzed state of the protein with modified heme, the heme changes its geometry from six-coordinate to five-coordinate and the equilibrium structure of the heme becomes domed instead of planar. However, the equilibrium structure of the heme in His93Gly mutant is still approximately planar, since it becomes four-coordinate following CO photolysis. The equilibrium bonds and angles are different for the photolyzed and nonphotolyzed states. They were changed “instantaneously” within the 2 fs integration time step upon the simulated photon absorption and ligand photolysis.

**2.3. A Measure of the Rate of Local Kinetic Energy Relaxation.** The ergodic measure is a useful means of determining the time scale for the self-averaging of a given property in a many-body system.<sup>32,4,25</sup> The fluctuation metric is defined by

$$\Omega(t) = \sum_j^N [f_j(t) - \bar{f}(t)]^2 \quad (1)$$

where  $f_j(t)$  is the time average for atom  $j$  of property  $F(t)$  of the system and  $\bar{f}(t)$  is the average over all  $N$  atoms of property  $F(t)$  at time  $t$ . Here we define  $f_j(t)$  to be the kinetic energy of the  $j$ th atom. If the total system is self-averaging and ergodic, the function  $\Omega_{KE}(t)$  will decay to zero asymptotically in time as

$$\frac{\Omega_{KE}(t)}{\Omega_{KE}(0)} \sim \frac{1}{D_{KE}t} \quad (2)$$

The slope of  $\Omega_{KE}(0)/\Omega_{KE}(t)$  is proportional to the generalized diffusion constant  $D_{KE}$  for the kinetic energy. The mean square of the fluctuations in the kinetic energy metric is related to this generalized diffusion constant  $D_{KE}$  that is a measure of the rate of the exploration in the momentum space.

If we assume that the microscopic motion is well described by a Langevin dynamics, one can relate the rate of self-averaging of kinetic energy to the magnitude of the static friction of a Langevin model. From the kinetic energy metric and the Langevin equation, one can identify the generalized associated diffusion constant of

$$D_{KE} = \gamma_0 \quad (3)$$

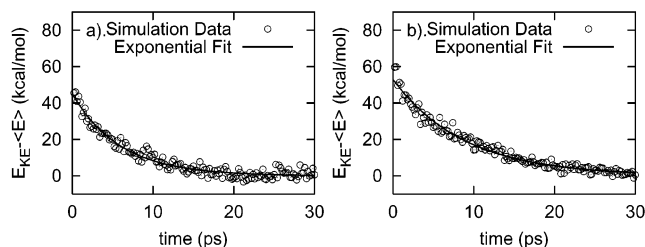


**Figure 2.** Clear demonstration of the single-exponential decay of the kinetic energy excess in the heme following ligand photolysis. The simulation data are represented by points; the best single-exponential fit is represented by the solid line. The time decay is modeled well by a single-exponential function with relaxation time (a) 5.9 ps for His93Gly mutant and (b) 8.8 ps for modified heme myoglobin.  $E_{KE}$  is the kinetic energy of the heme at time  $t$ .  $\langle E \rangle$  is the average equilibrium kinetic energy for the heme at 300 K, computed as  $3Nk_B T/2$ , where  $N$  is the number of atoms in the heme.

where  $\gamma_0$  is the static friction.<sup>25</sup> It follows that at long times

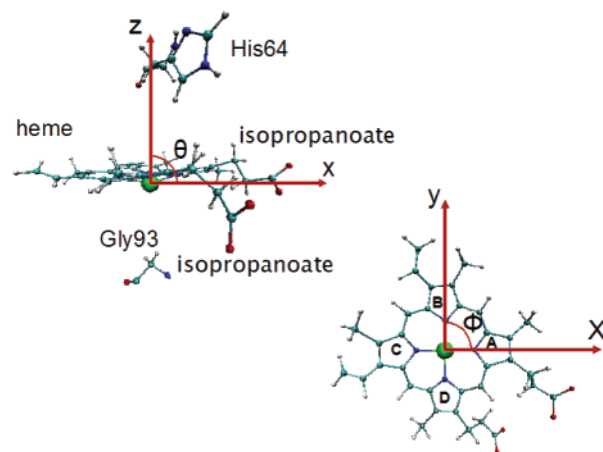
$$\text{slope} \left[ \frac{\Omega_{KE}(0)}{\Omega_{KE}(t)} \right] = \gamma_0 \quad (4)$$

### 3. Results and Analysis

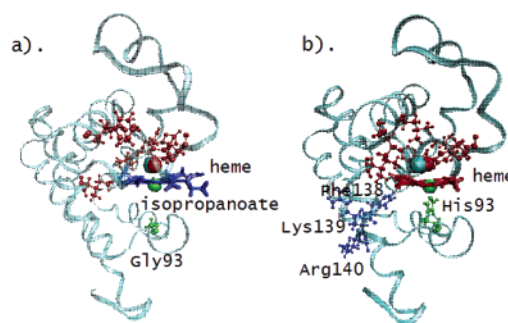
The simulated dynamical trajectories were used to determine the time scales and pathways of the kinetic energy relaxation following the absorption of a photon in modified myoglobin. The results for the mechanism and time scale of relaxation were compared with previous results for wild-type sperm whale myoglobin with heme *b*.

**3.1. Relaxation in His93Gly Mutant Myoglobin.** The average kinetic energy deposited over the 73 atoms in the heme of His93Gly mutant myoglobin during the excitation process is approximately 88 kcal/mol. Assuming complete intramolecular vibrational energy relaxation, the deposited energy will induce a change of over 400 K in the temperature of the heme. The average time dependence of the excess kinetic energy decay in the heme is shown in Figure 2a. The simulation data are well fitted by a single exponential decay function with the relaxation time 5.9 ps, which is in agreement with the time scale for heme “cooling” for photolyzed wild-type myoglobin.<sup>26</sup> From this evidence, we conclude that the covalent bond to the heme does not play a primary role in the process of heme “cooling” for myoglobin in room temperature aqueous solution.

**3.2. Pathways for the Kinetic Energy Relaxation in His93Gly Mutant Myoglobin.** The analysis of the pathways for energy relaxation is made nontrivial by the large number of accepting modes. While the absolute excess energy that must dissipate is large, the average mode accepts a quantity of energy less than the thermal energy  $k_B T$ . That observation supports the applicability of a classical weak collision model of energy transfer and relaxation.<sup>25</sup> Here we employed the analysis methods of Sagnella and Straub<sup>26</sup> to investigate the possible pathways of energy transfer—the “mechanism” of heme “cooling”. The coordinates of the system were translated and rotated so that the Fe atom was the origin while two nitrogen atoms of the heme’s pyrrole rings A and B were arranged along the  $x$ -axis and  $y$ -axis, respectively. This transformation results in the Fe atom and the four pyrrole nitrogens staying more or less in the  $x$ - $y$  plane. Figure 3 illustrates the orientation of the heme with respect to the angles  $\theta$  and  $\phi$ .  $\theta$  is the angle between the  $z$ -axis and the  $x$ - $y$  plane;  $\phi$  is the angle measuring the rotation of the heme plane about the  $z$ -axis. Using this definition, the four pyrrole ring nitrogens were located near  $\theta = 90^\circ$  and  $\phi$  values of  $0^\circ$ ,  $90^\circ$ ,  $180^\circ$ , and  $270^\circ$  for ring A, B, C, and D, respectively.



**Figure 3.** The heme in His93Gly mutant myoglobin with its Fe atom at the origin and nitrogen atoms of pyrrole heme rings A and B located along the  $x$ -axis and  $y$ -axis, respectively. The Fe atom and the four nitrogen atoms are to a good approximation in the  $x$ - $y$  plane during the simulated dynamics.  $\theta$  is the angle between the  $z$ -axis and the  $x$ - $y$  plane;  $\phi$  is the angle measuring the rotation of the heme plane about the  $z$ -axis.



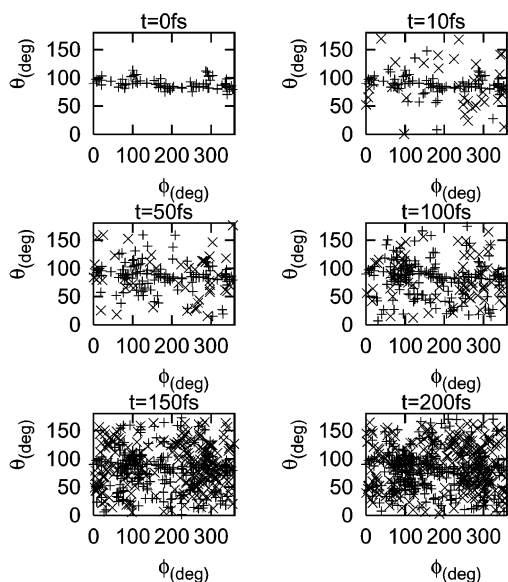
**Figure 4.** Hot protein residues in (a) His93Gly mutant myoglobin and (b) modified heme myoglobin depicted using space-filling CPK models. (a) Red indicates the heme pocket region, green indicates the proximal Gly93 residue, and blue identifies the specific energy “funneling” channel involving the heme isopropanoate side chains. (b) Red indicates the heme pocket region, green indicates the proximal His93 residue, and blue identifies the specific “through space” energy transfer channel involving Phe138, Lys139, and Arg140.

Figure 4a depicts the positions of the “hot” protein residues—those residues with excess kinetic energy significantly larger than their equilibrium average values. The hot protein residues, shown in the space-filling CPK model, are those excited by direct collisions with the vibrationally excited heme atoms and CO molecule. It is apparent that in the absence of the covalent bond of the His93 to the heme iron, as in its presence, the dominant channel of energy flow out of the heme is through the heme’s two isopropanoate side chains.

In Figure 5, there are six snapshots at different times showing the positions (in  $\theta$  and  $\phi$ ) of atoms with excess kinetic energy that is significantly higher than the equilibrium average value. Both protein atoms and solvent atoms are shown. There is a high concentration of kinetic energy—a “hot spot” in the region of  $\theta = 90^\circ$   $\phi = 300^\circ$ —that is the location of the two isopropanoate side chains. This plot clearly shows the directed “funneling” of kinetic energy from the heme through its side chains into the surrounding solvent. These simulation results are consistent with the results of the earlier computational study by Sagnella and Straub of wild-type myoglobin.<sup>26</sup>

**3.3. Relaxation in Modified Heme Myoglobin.** The average kinetic energy deposited over the 57 atoms in the heme during the excitation process is 88 kcal/mol, which leads to an increase





**Figure 5.** Distribution of the hot atoms with a significantly higher kinetic energy than the mean value at the equilibrium temperature in His93Gly mutant myoglobin. Red (+) represents the protein atoms, and blue (x) indicates the solvent atoms.

of over 500 K in the temperature of the heme. The average time dependence of the excess kinetic energy decay in the heme is shown in Figure 2b. The simulation data are well fitted by a single exponential decay function with the relaxation time 8.8 ps. There is no evidence of biexponential or stretched exponential time relaxation. In previous work, the time scale for heme “cooling” was found to be 5.9 ps for photolyzed wild-type myoglobin. Therefore, it is observed that the rate of kinetic energy relaxation of the heme decreased by 50% relative to the native wild-type myoglobin due to the amputation of the heme’s two isopropionate side chains. These results are strong evidence that the two isopropionate side chains play an important role in “funneling” excess kinetic energy from the heme of wild-type myoglobin.

**3.4. Pathways for the Kinetic Energy Relaxation in Modified Heme Myoglobin.** Figure 4b depicts the positions of the “hot” protein residues in modified heme mutant myoglobin. The hot protein residues, shown in the space-filling CPK model, are found in two distinct regions. The red region consists of those residues forming the heme pocket. Those atoms are excited by direct collisions with the vibrationally excited heme atoms and the photolyzed CO molecule. The blue region can be recognized as a specific “through space” energy transfer channel that involves residues Phe138, Lys139, and Arg14. The distance between the ethyl side chain of the heme and the phenyl group of Phe138 is short, making collisions between the heme side chains and the phenyl group common. The average distance between the carbon atoms of the ethyl side chain and the closest carbon atoms of the phenyl group in Phe138 is 4.0 Å. The polar Lys139 and Arg140 residues extend out of the protein and are highly solvated. The  $\phi$  value is 100° for this specific energy transfer channel.

Figure 6 shows the distribution of hot water molecules along  $\phi$ . Although it is not obvious, we can distinguish a high concentration of kinetic energy in the region of  $\phi = 100^\circ$ , which is the location of the side chain in the heme’s B pyrrole ring. This suggests that kinetic energy is transferred from the side chain B of the heme to the solvent directly. However, since the kinetic energy must pass two or three peptide bonds along this pathway, in order to reach the solvent, this energy transfer

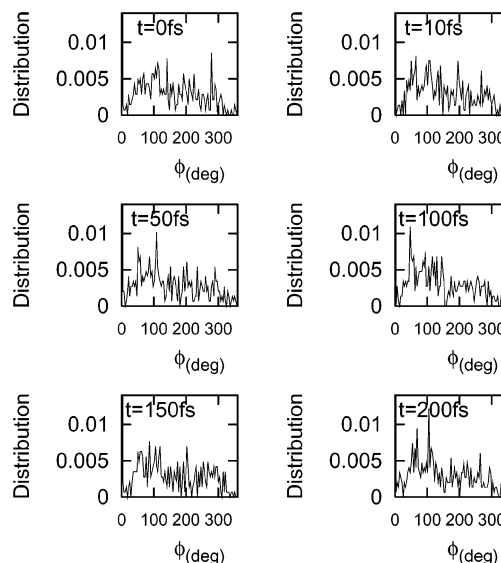


**Figure 6.** Distribution of hot water molecules along  $\phi$  in modified heme myoglobin.

channel is not as effective or, consequently, important as the “highly directly energy funneling” found previously in myoglobin. We imagine that this pathway is a competing secondary pathway in myoglobin. We find that it is also a secondary energy transfer channel in the modified myoglobin.

In summary, the spreading of the kinetic energy from the heme to the protein occurs through three channels. The first is the “through projectile” energy transfer by ligand collisions with the heme pocket residues, including Leu29, Leu32, Phe43, Val68, His64, and Ile107. In the photolyzed state, the heme interacts with the CO molecule through nonbonded interactions. The excess energy in the CO ligand is transferred to the heme pocket residues through direct collisions. It should be noted that the “through projectile” energy transfer channel only occurs on a subpicosecond time scale immediately following photolysis. After only a few collisions with its neighbor atoms, CO will begin to dissipate its excess kinetic energy via the “through space” channel. The second channel is “through bond” energy transfer. The proximal His93 is the only residue that is covalently bonded to the heme. The excess kinetic energy could be transferred through the intramolecular vibrational relaxation. The third energy transfer channel is “through space” energy transfer due to direct collisions between the hot heme atoms and the surrounding protein atoms, most importantly Phe138, Lys139, and Arg140, and solvent molecules.

**3.5. Spatial Anisotropy in Kinetic Energy Relaxation.** The inverse kinetic energy fluctuation metric  $\Omega_{KE}(0)/\Omega_{KE}(t)$  was computed as a function of time for the total system, the protein, the heme, and the solvent. Each data set consists of an average over ten 30 ps trajectories. The effective intrinsic friction constants,  $\gamma_0$ , were derived using eq 4. In Figure 7, the function  $\Omega_{KE}(t)$  for the solvated modified myoglobin system is depicted. While the rate of convergence is significantly slower in the heme, after 20 ps it appears that there is effective self-averaging of the kinetic energy by the heme, protein, and solvent.

In Figure 8, the function  $\Omega_{KE}(0)/\Omega_{KE}(t)$  for the solvated modified myoglobin system is plotted as a function of time. Data for the individual contributions of the protein, the heme, and the solvent are listed in Table 1. These data illustrate the relative amount of damping felt by the atoms within the indicated subsets of the solvated modified myoglobin system. The frictional forces felt by the heme and solvent atoms are

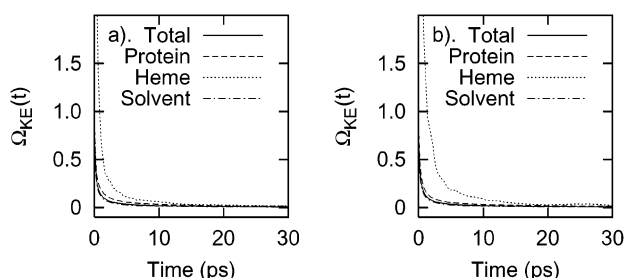


**Figure 7.**  $\Omega_{KE}(t)$  plotted as a function of time for the solvated system: the protein, the heme, and the solvent in (a) His93Gly mutant myoglobin and (b) modified heme myoglobin. The ergodicity criterion requires  $\Omega_{KE}(t)$  to decay to zero with time. The calculation was averaged over the 10 trajectories.

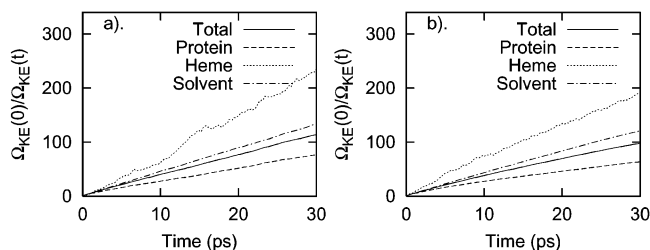


**Figure 8.**  $\Omega_{KE}(0)/\Omega_{KE}(t)$  plotted as a function of time for the solvated protein system: the protein, the heme, and the solvent in (a) His93Gly mutant myoglobin and (b) modified heme myoglobin. The calculated values represent averages over the 10 trajectories.

**TABLE 1: Time Scales for the Convergence of the Kinetic Energy Metric and Static Friction in His93Gly Mutant Myoglobin and Modified Heme Myoglobin<sup>a</sup>**

region	$\gamma_0$ (ps <sup>-1</sup> )		$1/\gamma_0$ (ps)	
	His93Gly	modified heme	His93Gly	modified heme
total	$3.83 \pm 0.10$	$3.30 \pm 0.30$	$0.26 \pm 0.01$	$0.30 \pm 0.03$
protein	$2.62 \pm 0.18$	$2.24 \pm 0.11$	$0.38 \pm 0.03$	$0.45 \pm 0.02$
heme	$6.37 \pm 1.05$	$6.09 \pm 2.31$	$0.16 \pm 0.03$	$0.16 \pm 0.06$
solvent	$4.47 \pm 0.10$	$4.15 \pm 0.10$	$0.22 \pm 0.01$	$0.24 \pm 0.01$

<sup>a</sup> Here “total” means the entire system consisting of the modified myoglobin, the heme, and solvent.

considerably higher than those in the remainder of the system. The time constants calculated as the reciprocal intrinsic friction for the protein, the heme, and the solvent are 0.38, 0.16, and 0.22 ps, respectively, for His93Gly mutant myoglobin, and 0.45, 0.16, and 0.24 ps, respectively, for modified heme myoglobin. The topological structure of heme and protein are different in these two systems. The heme is four-coordinate planar in the His93Gly mutant myoglobin and five-coordinate domed in the modified heme mutant. In each of the systems, the time scales for the protein, heme, and solvent relaxation are all larger in the modified heme myoglobin. These results suggest that the solvent degrees of freedom play a significant role as acceptor modes in the flow of energy out of the heme that effects not only the rate of kinetic energy equipartitioning in the heme but the rate of equipartitioning in the protein and solvent as well.

#### 4. Summary and Conclusions

This work has investigated the time scales and pathways of vibrational energy relaxation in two modified forms of myoglobin following ligand photolysis. Our simulation results suggest that the excess kinetic energy of the heme dissipates according to a single exponential decay process with the relaxation time constant of 5.9 ps for the His93Gly mutant and 8.8 ps for the modified heme mutant. The rate of heme

vibrational energy relaxation in wild-type myoglobin with heme *b* was found to be 5.9 ps<sup>26</sup> by simulation, in agreement with the 6.2 ps time scale measured experimentally by Anfinrud and co-workers.<sup>12</sup>

In more recent studies, Kitagawa, Haruta, and Mizutani have observed relaxation of vibrationally excited heme in photodissociated MbCO on the time scale of 1–2 ps, derived by monitoring the anti-Stokes Raman intensity.<sup>33</sup> Champion and co-workers have observed the vibrational relaxation of selected heme modes in MbO<sub>2</sub> and MbNO on the time scale of 1 ps, for the six-coordinate heme, and biphasic decay in 0.5 and 2.4 ps, in the five-coordinate deoxy heme.<sup>34</sup> In our study, we observe the “cooling” of the five-coordinate heme on a time scale 2–3 times longer than indicated by these studies. This may be due to the fact that their estimates are based on measurements of the time evolution of the Soret peak<sup>34</sup> or anti-Stokes Raman intensity,<sup>33</sup> while we monitor a more complete thermal relaxation of the heme as a whole.

The cleavage of the single covalent bond between the heme and apoprotein in myoglobin does not cause any change in the rate or mechanism of vibrational energy relaxation of the heme. However, the amputation of the heme’s isopropionate side chains results in an increase in the vibrational energy relaxation time by 50%. There is a corresponding change in the mechanism of heme “cooling” with a significant pathway for energy flow being “through space” energy transfer from the heme to neighboring protein side chains. Our results support the conjecture that the two isopropionate side chains and their coupling to the solvent bath play a dominant role in the dissipation of excess kinetic energy of the excited heme in solvated wild-type myoglobin.

**Acknowledgment.** We are most grateful to Prof. T. Kitagawa for stimulating discussions. We thank Prof. R. J. D. Miller and Prof. P. Champion for helpful comments. We are thankful for the generous support of this research by the National Science Foundation (CHE-9975494 and CHE-0316551).

#### References and Notes

- (1) Elber, R.; Karplus, M. *Science* **1987**, *235*, 318–321.
- (2) Elber, R.; Karplus, M. *J. Am. Chem. Soc.* **1990**, *112*, 9161–9175.
- (3) Straub, J.; Karplus, M. *Chem. Phys.* **1991**, *158*, 221–248.
- (4) Straub, J.; Rashkin, A.; Thirumalai, D. *J. Am. Chem. Soc.* **1994**, *116*, 2049–2063.
- (5) Zewail, A. *J. Phys. Chem.* **1996**, *100*, 12701–12712.
- (6) Li, H.; Elber, R.; Straub, J. *J. Biol. Chem.* **1993**, *268*, 17908–17916.
- (7) Meller, J.; Elber, R. *Biophys. J.* **1998**, *74*, 789–802.
- (8) Miller, R. J. D. *Annu. Rev. Phys. Chem.* **1991**, *42*, 581–614.
- (9) Miller, R. J. D. *Can. J. Chem.* **2002**, *80*, 1–24.
- (10) Mizutani, Y.; Kitagawa, T. *Science* **1997**, *278*, 443–446.
- (11) Mizutani, Y.; Kitagawa, T. *Bull. Chem. Soc. Jpn.* **2002**, *75*, 623–639.
- (12) Lim, M.; Jackson, T.; Anfinrud, P. *J. Phys. Chem.* **1996**, *100*, 12043–12051.
- (13) Sagnella, D.; Straub, J. *Biophys. J.* **1999**, *108*, 70–84.
- (14) Sagnella, D.; Straub, J.; Jackson, T.; Lim, M.; Anfinrud, P. *Proc. Natl. Acad. Sci. U.S.A.* **1999**, *96*, 14324–14329.
- (15) Hill, J.; Dlott, D.; Rella, C.; Peterson, K.; Decatur, S.; Boxer, S.; Fayer, M. *J. Phys. Chem.* **1996**, *100*, 12100–12107.
- (16) Ma, J.; Huo, S.; Straub, J. *J. Am. Chem. Soc.* **1997**, *119*, 2541–2551.
- (17) Okazaki, I.; Hara, Y.; Nagaoka, M. *Chem. Phys. Lett.* **2001**, *337*, 151–157.
- (18) Asplund, M.; Zanni, M.; Hochstrasser, R. *Proc. Natl. Acad. Sci. U.S.A.* **2000**, *97*, 8219–8224.
- (19) Kholodenko, Y.; Volk, M.; Gooding, E.; Hochstrasser, R. *Chem. Phys.* **2000**, *259*, 71–87.
- (20) Henry, E.; Eaton, W.; Hochstrasser, R. *Proc. Natl. Acad. Sci. U.S.A.* **1986**, *83*, 8982–8986.

- (21) Lian, T.; Locke, B.; Kholodenko, Y.; Hochstrasser, R. *J. Phys. Chem.* **1994**, *98*, 11648–11656.
- (22) Petrich, J. W.; Poyart, C.; Martin, J. L. *Biochemistry* **1988**, *27*, 4049–4060.
- (23) Lingle, R.; Xu, X.; Zhu, H.; Yu, S. C.; Hopkins, J. B. *J. Phys. Chem.* **1991**, *95*, 9320–9331.
- (24) Li, P.; Sage, J.; Champion, P. *J. Chem. Phys.* **1992**, *97*, 3214–3227.
- (25) Sagnella, D.; Straub, J.; Thirumalai, D. *J. Chem. Phys.* **2000**, *113*, 7702–7711.
- (26) Sagnella, D.; Straub, J. *J. Phys. Chem. B* **2001**, *105*, 7057–7063.
- (27) Brooks, B.; Bruccoleri, R.; Olafson, B.; States, D.; Swaminathan, S.; Karplus, M. *J. Comput. Phys.* **1983**, *4*, 187–217.
- (28) MacKerell, A. D., Jr.; Bashford, D.; Bellott, M.; Dunbrack, R. L., Jr.; Evanseck, J.; Field, M.; Fischer, S.; Gao, J.; Guo, H.; Ha, S.; Joseph-McCarthy, D.; Kuchnir, L.; Kuczera, K.; Lau, F.; Mattos, C.; Michnick, S.; Ngo, T.; Nguyen, D.; Prodhom, B.; Reiher, W. III; Roux, B.; Schlenkrich, M.; Smith, J.; Stote, R.; Straub, J. [E.]; Watanabe, M.; Wiorkiewicz-Kuczera, J.; Yin, D.; Karplus, M. *J. Phys. Chem. B* **1998**, *102*, 3586–3616.
- (29) Verlet, L. *Phys. Rev.* **1967**, *159*, 98–103.
- (30) Tuckerman, M.; Berne, B.; Martyna, G. *J. Chem. Phys.* **1992**, *97*, 1990–2001.
- (31) Frenkel, D.; Smit, B. *Understanding molecular simulation: from algorithms to applications*, 2nd ed.; Academic Press: New York, 2001.
- (32) Thirumalai, D.; Mountain, R. *Phys. Rev. A* **1990**, *42*, 4574–4587.
- (33) Kitagawa, T.; Haruta, N.; Mizutani, Y. *Biopolymers* **2002**, *67*, 207–213.
- (34) Ye, X.; Demidov, A.; Champion, P. *J. Am. Chem. Soc.* **2002**, *124*, 5914–5924.